

X-RAY OPTICS

DOI: 10.1070/QEL16177

X-ray reduction imaging of inclined reflective masks at critical angles

I.A. Artyukov, A.S. Busarov, A.V. Vinogradov, N.L. Popov

Abstract. **We have proposed and simulated optical schemes for producing reduced images by X-ray lasers or harmonic generators at a wavelength of ~14 nm. The mask in this case is placed at a small angle to the optical axis, corresponding to the angle of total external reflection of the material. We have determined the optimal position of the detector (resist) and the corresponding spatial resolution. The results can be used to solve problems in nanotechnology and nanostructuring of surfaces.**

Keywords: *X-ray lithography, extreme ultraviolet, coherent optics and microscopy.*

1. Introduction

Reduced-scale printing and photolithography are important methods for nanotechnology and nanoelectronics [1, 2]. In many cases, they pattern a reduced image of a mask by placing it on a photoresist layer atop a functional material. The quest for nanopattering actualises the use of radiation with increasingly shorter wavelengths, which have now reached 13 nm [3–5]; in addition, a 6.7-nm EUV lithography source is discussed [6]. Due to high absorption, the use of transmission masks in this range and for shorter wavelengths is problematic. At the same time, it is known that high-resolution images are obtained using normal incidence optics, when samples are illuminated at right angles to the surface, which results in fabricating reflective multilayer-coated mask blanks [7]. However, the mirror reflectance at normal incidence decreases sharply with decreasing wavelength below 6 nm [8]. The purpose of this work is to study the possibility of producing reduced images of reflective masks illuminated at grazing incidence angles that are close to the angles of the total external reflection, including hard X-rays.

2. Two-dimensional geometry

X-rays are reflected from the sample surface at grazing angles that are smaller than the critical angle. Therefore, the optical system should provide, in addition to the similarity of the object and the image, a large enough angle of incidence on the detector (otherwise, light will be reflected from the detector) at a small angle of reflection from the object.

I.A. Artyukov, A.S. Busarov, A.V. Vinogradov, N.L. Popov P.N. Lebedev Physics Institute, Russian Academy of Sciences, Leninsky prosp. 53, 119991 Moscow, Russia; e-mail: albusarov@mail.ru

Received 6 July 2016
Kvantovaya Elektronika **46** (9) 839–844 (2016)
Translated by I.A. Ulitkin

If the object is inclined to the optical axis of the system, the image is also obtained on an inclined plane that is optically conjugated with the object. In particular, in a two-dimensional geometry the object and the image are arranged on one ray passing through the optical system (ABC beam in Fig. 1). In the case of reduced-scale printing (lithography), the angle of incidence to the optical axis increases. Let us illustrate this in the language of the paraxial wave optics in the case of an ideal optical system in a two-dimensional geometry. To do this, we will carry out a wave theory analysis of imaging of an inclined object in the optical system*.

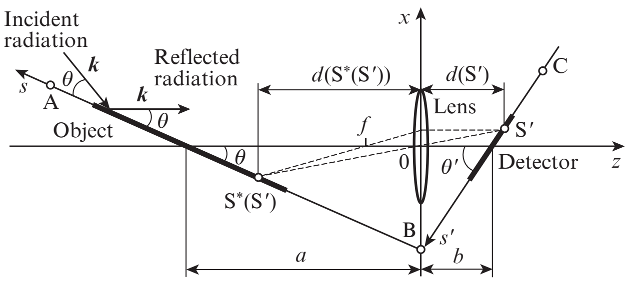

Figure 1. Scheme of the optical system:
θ, θ' are the angles of inclination of the object and image (detector) planes, respectively, to the z axis; a is the distance from the object to the lens; b is the distance from the lens to the image; $\boldsymbol{k}$ is the wave vector; $S^*(S')$ is the preimage of point S'; $d(S')$ is the distance from point S' to the x axis; $d(S^*(S'))$ is the distance from point $S^*(S')$ to the x axis.

Let us consider the spatial harmonics $\exp(iqs)$ in the object plane (Fig. 1), described by the equations

$$x = s\sin\theta,$$
$$z = -a - s\cos\theta, \tag{1}$$

and determine the field produced by it behind the lens, using a parabolic wave equation

$$\frac{\partial^2 u(x,y)}{\partial x^2} + 2ik\frac{\partial u(x,z)}{\partial z} = 0. \tag{2}$$

Its solution with the boundary conditions set on an inclined object is

* Rigorous analysis has been made in our papers [9, 10]. The standard case of a vertical object is described in monograph [11].

$$u_1(x,z) = \left[\mathrm{i}\alpha(q)x - \mathrm{i}\frac{\alpha^2(q)}{2k}(z+a)\right], \tag{3}$$

$$u_1(x = s\sin\theta,\, z = -a - s\cos\theta) = \exp(\mathrm{i}qs), \tag{4}$$

where $\alpha(q)$ is defined by the equation

$$\alpha(q)\sin\theta + \frac{\alpha^2(q)}{2k}\cos\theta = q. \tag{5}$$

The action of an ideal lens can be described by a phase factor $T(x) = \exp[-\mathrm{i}kx^2/(2f)]$, where f is the focal length, so that on the right side of the lens, the field has the form

$$u_2(x, z=0) = u_1(x, z=0)T(x). \tag{6}$$

Within the framework of the paraxial approximation, the field on the right side of the lens can be found using the Fresnel integral:

$$u_2(x,z) = \sqrt{k/(2\pi \mathrm{i}z)}\int_{-\infty}^{\infty}\mathrm{d}x' u_2(x', z=0) \times \exp\left[\frac{\mathrm{i}k(x-x')^2}{2z}\right]. \tag{7}$$

Substituting (3) into (6), and then the result into (7), calculating the integral and performing elementary transformations, we obtain

$$u_2(x,z) = \frac{1}{\mathrm{i}\sqrt{z/f-1}}\exp\left[\mathrm{i}\frac{kx^2}{2f(z/f-1)}\right] \times\exp\left\{\frac{\mathrm{i}}{z/f-1}\left[-\alpha(q)x - \frac{\alpha^2(q)}{2k}a\left(\frac{1}{f}-\frac{1}{a}\right)\left(z - \frac{1}{1/f-1/a}\right)\right]\right\}. \tag{8}$$

We rewrite (5) as follows:

$$\alpha(q) = \frac{q}{\sin\theta} - \frac{\alpha^2(q)}{2k}\frac{1}{\tan\theta}. \tag{9}$$

Substituting (9) into (8), we obtain

$$u_2(x,z) = \exp\left[\mathrm{i}\frac{kx^2}{2f(z/f-1)}\right](\mathrm{i}\sqrt{z/f-1})^{-1} \times \exp\left\{\frac{\mathrm{i}}{z/f-1}\left\{-\frac{qx}{\sin\theta} + \frac{\alpha^2(q)}{2k\tan\theta} \times\left[x - a\left(\frac{1}{f}-\frac{1}{a}\right)\tan\theta\left(z - \frac{1}{1/f-1/a}\right)\right]\right\}\right\}. \tag{10}$$

Expression (10) defines the field behind the lens in a form suitable for further consideration.

Let us now find the image, i.e. the field on a plane optically conjugated with the object plane. As noted in Introduction, in the two-dimensional geometry this is the ABC beam (Fig. 1). Its equation behind the lens has the form:

$$x - (z-b)\tan\theta' = 0, \tag{11}$$

where

$$\frac{1}{a}+\frac{1}{b}=\frac{1}{f};\quad \tan\theta' = \frac{1}{M_0}\tan\theta;\quad M_0 = \frac{b}{a}. \tag{12}$$

The equation for the plane (11) can be written in the parametric form:

$$x(s') = -s'\sin\theta',\qquad z(s') = b - s'\cos\theta'. \tag{13}$$

Let us substitute the parametric equation (13) into (10); in this case, the coefficient at $\alpha^2(q)$ in the exponent in (10) will be, with allowance for (12), equal to zero, and as a result we obtain

$$u(s') = u_2(x(s'), z(s')) = \exp\left\{\mathrm{i}\frac{kx^2(s')}{2f\,[z(s')/f-1]}\right\} \times[\mathrm{i}\sqrt{z(s')/f-1}]^{-1}\exp\left\{\frac{\mathrm{i}qs'}{[z(s')/f-1]\sin\theta/\sin\theta'}\right\}. \tag{14}$$

Thus, the field of the object, specified in the form of the harmonic $\exp(\mathrm{i}qs)$, transforms into the field (14). Consequently, in the image plane the field of an arbitrary object

$$u_0(s) = \int_{-\infty}^{\infty}\mathrm{d}q U_0(q)\exp(\mathrm{i}qs) \tag{15}$$

transforms into the expression

$$u(s') = \exp\left[\mathrm{i}\frac{kx^2(s')}{2fQ(s')}\right][\mathrm{i}\sqrt{Q(s')}]^{-1}u_0(s^*(s')), \tag{16}$$

where

$$s^*(s') = \frac{s'}{Q(s')\sin\theta/\sin\theta'};\quad Q(s') = \frac{z(s')}{f} - 1. \tag{17}$$

Formula (16) – the main result of this section – shows that the inclined object and its image are located on the same ray passing through the optical system. It is a direct result of the expression for the field behind the lens (10).

The expression for the intensity in the image plane $I(s') = |u(s')|^2$ will have the form

$$I(s') = \frac{1}{Q(s')}I_0(s^*(s')), \tag{18}$$

where $I_0(s^*(s'))$ is the intensity in the object plane.

It can be shown that $S^*(S')$ is a preimage of point S' on an object, produced according to the laws of geometrical optics (Fig. 1). Let us also explain the geometric meaning of $Q(s')$. It is easy to show that $Q(s')$ is the ratio of two distances:

$$Q(s') = \frac{d(s')}{d(s^*(s'))}, \tag{19}$$

where $d(s')$ and $d(s^*(s'))$ are the distances from point S' and its conjugated point $S^*(S')$ to the lens (Fig. 1). With the help of relations (12), (13) and (18), we can obtain the equation:

$$Q(s') = \frac{M_0}{1 + [s^*(s')/f]M_0\cos\theta}. \tag{20}$$

Let the distribution of the object intensity $I_0(s)$ be given near the optical axis for $s \in (-s_0, s_0)$; in this case, it makes sense to consider such s', so that $s^*(s') \in (-s_0, s_0)$. Then, when the condition

$$\frac{s_0}{f} M_0 \ll 1 \quad (21)$$

is fulfilled, taking into account equality (20) and the first formula in (17), we can estimate

$$Q(s') \approx M_0, \quad s^*(s') \approx \frac{s'}{M_0 \sin\theta / \sin\theta'}. \quad (22)$$

In this case, we can write (18) in the form

$$I(s') = \frac{1}{M_0} I_0\left(\frac{s'}{M(\theta)}\right), \quad (23)$$

where the magnification factor

$$M(\theta) = M_0 \sqrt{1 + (M_0^2 - 1)\cos^2\theta}, \quad (24)$$

because, as can be easily found, using the second relation in (12),

$$\frac{\sin\theta}{\sin\theta'} = \sqrt{1 + (M_0^2 - 1)\cos^2\theta}. \quad (25)$$

As can be seen from formula (23), the image is similar to the object.

3. Three-dimensional case

One can see that in a three-dimensional geometry (Fig. 2), the corresponding expression (18) has the form

$$I(s', y') = \frac{1}{Q^2(s')} I_0\left(s^*(s'), \frac{y'}{Q(s')}\right). \quad (26)$$

The derivation of (26) is presented in the Appendix. In expression (26), the distributions $I(s', y')$ and $I_0(s, y)$ correspond to the intensities in the image and object planes, and the quantities $s^*(s')$ and $Q(s')$ coincide with those given in (17).

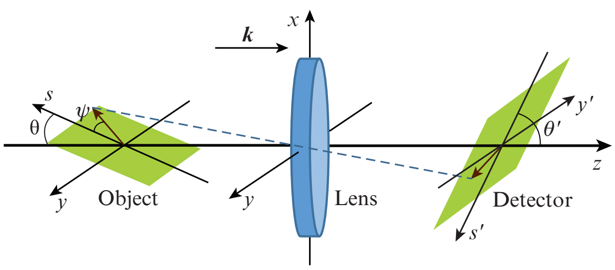

Figure 2. Scheme of the optical system for the three-dimensional case.

If the object intensity distribution $I_0(s, y)$ is set near the optical axis for $s \in (-s_0, s_0)$, then, when condition (21) is fulfilled, our estimation (22) is valid and expression (26) can be written as

$$I(s', y') = \frac{1}{M_0^2} I_0\left(\frac{s'}{M(\theta)}, \frac{y'}{M_0}\right), \quad (27)$$

where $M(\theta)$ is determined by (24). Thus, the magnification factor is equal to $M(\theta)$ along the s' axis and to M_0 along the y' axis. We also present a formula for $M(\theta, \psi)$ – the magnification factor in the direction specified in the object plane by the angle ψ (Fig. 2):

$$M(\theta, \psi) = M_0 \sqrt{1 + (M_0^2 - 1)\cos^2\theta \cos^2\psi}. \quad (28)$$

Formulas (27) and (28) generalise expressions (23) and (24) to the three-dimensional case.

4. Reduction imaging. Lithography

Formulas and conclusions of Sections 2 and 3 can be applied to lithography [$M(\theta) < 1$] and microscopy [$M(\theta) > 1$]. The essential difference between them is the grazing angle of the beam relative to the recording medium. In lithography, it increases ($\theta' > \theta$), and in microscopy it decreases ($\theta' < \theta$). As noted above, this creates an additional problem. Indeed, radiation is incident on the detector at angles smaller than the angles onto the object, and therefore, it will be reflected rather than absorbed. This problem requires special consideration. In our work, we restrict ourselves to the tasks of lithography and nanostructuring [$M(\theta) < 1$], referring to the use of coherent sources at a wavelength of ~13 nm. This range is now mastered by laboratory X-ray lasers [12] and by harmonic generators of IR lasers [13], and we can talk about the experimental testing of the proposed method.

Let us present the results of calculation of the optical system providing us with the effective reflection of radiation at $\lambda = 13.9$ nm from the mask and at the same time close-to-normal incidence of radiation on the detector, as well as find its resolution.

The following parameters were used: the angle of incidence on the mask, $\theta = 0.140$ rad (the angle of reflection from the mask is the same); the focal distance of the lens, $f = 1$ mm; the distance from the lens of the mask centre, $a = 16.341$ mm; the distance from the lens to the image centre, $b = 1.065$ mm; the magnification factor $M(\theta) = 0.01$ in the direction of the s axis; the magnification factor $M_0 = 0.0652$ in the direction of the y axis; the angle of incidence on the detector, $\theta' = 1.14$ rad; and the mask with the size 500×500 μm consisting of five rectangular strips (Fig. 3) ($s_0 = 250$ μm).

As a result of numerical simulation we obtained an image, shown in Fig. 4, which does not contain noticeable distortions of the object shape and intensity distribution.

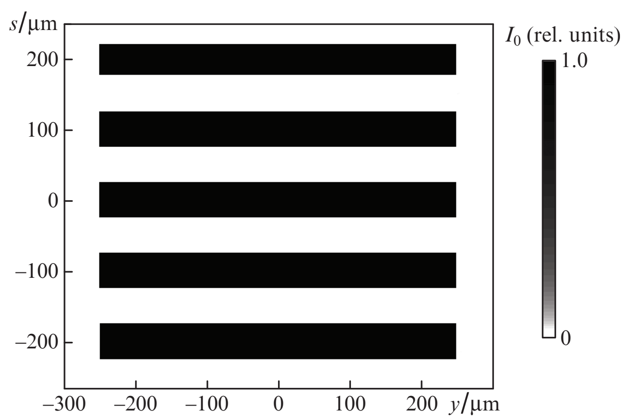

Figure 3. Intensity distribution of a test object.

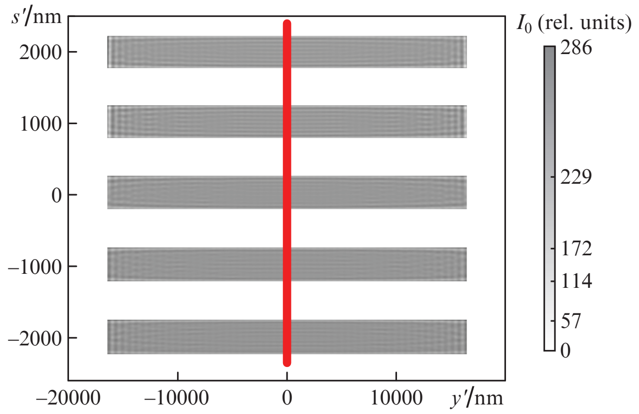

Figure 4. Intensity distribution on the detector after the optical system (lens). The dependence in Fig. 5 corresponds to the vertical line.

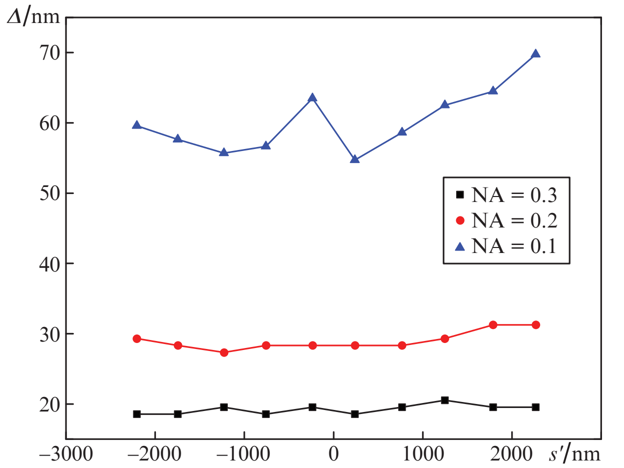

Figure 6. Resolution along the s' axis found by the 10%–90% method.

For a quantitative estimate of the resolution, we use the 90%–10% method. The intensity distribution in Fig. 5 corresponds to the vertical line in Fig. 4. Also, Fig. 5 shows two levels corresponding to the intensities of 10% and 90%. There are ten points of intersection of the intensity line with each of these levels. We denote the coordinates of these points by $s'_{i10\%}$ and $s'_{i90\%}$, where $i = 1-10$. Next, we plot the dependence of Δ on s' by ten points (Fig. 6), corresponding to the 'sides of the steps' in Fig. 5 (two 'sides' in each of the five 'steps'); in this case, $\Delta_i = |s'_{i10\%} - s'_{i90\%}|$, a $s'_i = (s'_{i10\%} + s'_{i90\%})/2$. The intensity in Fig. 5 is normalised to the doubled value of the average intensity.

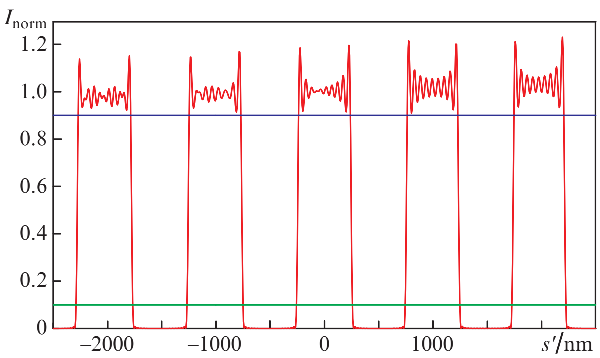

Figure 5. Normalised intensity distribution corresponding to the vertical line in Fig. 4.

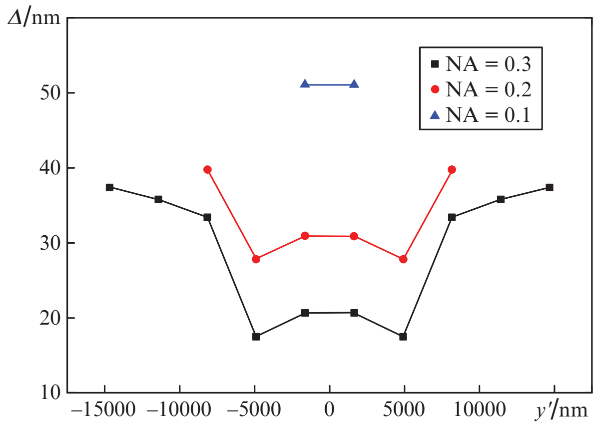

Figure 7. Resolution along the y' axis found by the 10%–90% method.

The value of Δ stands for resolution in this method. Thus, for the s' axis the resolution is $\Delta \approx 20$ nm at a value of the aperture NA = 0.3, about 30 nm at NA = 0.2 and about 60 nm at NA = 0.1, which agrees well with the known law $\Delta \propto 1/\text{NA}$ (as in all three cases $\Delta \cdot \text{NA} \approx 6$).

Similarly, we calculate the resolution of the scheme along the y axis (Fig. 7). For the y axis the resolution is $\Delta \approx 20$ nm at NA = 0.3, about 30 nm at NA = 0.2 and about 50 nm at NA = 0.1, which correlates well with the above expression $\Delta \propto 1/\text{NA}$.

Distortions introduced by a finite aperture lens may be divided into two types: firstly, uniform image blurring of an ideal lens, and secondly, a geometric shadow of the finite aperture. Figure 6 demonstrates only a uniform blur, while Fig. 7 presents both types of distortions. The analysis showed that the use of coherent radiation at a wavelength of 13.9 nm produces reduced images with the masks illuminated at grazing angles. In this case, it is possible to fabricate nanostructures with sizes down to 20–30 nm. Diffraction and inclination of the object do not introduce any visible distortions in the mask image.

5. Conclusions

Thus, we have proposed a new method of reflective mask lithography. It allows oblique illumination of a mask by a coherent beam at an angle that is less than a critical angle. The advantage of this method is the use of inclined masks in a wide range of wavelengths, in particular where normal incidence multilayer X-ray optics is not applicable; for example, in using a free electron laser in the wavelength range of 4–0.1 nm [14].

Acknowledgements. The authors thank A.V. Goncharskii for discussions.

The work was supported by the Basic Research Programme of the Presidium of the Russian Academy of Sciences 'Fundamental and applied problems of photonics and physics of new optical materials'.

Appendix

Acting similarly to the two-dimensional case, we consider the three-dimensional case. We define, as a product of the harmonics $u_0(s, y) = \exp(\mathrm{i}qs + \mathrm{i}py)$, the field in the object plane (see Fig. 2)

$$x = s\sin\theta, \qquad z = -a - s\cos\theta \tag{A1}$$

and determine the field produced by them behind the lens, using a parabolic wave equation, which in the three-dimensional case has the form

$$\frac{\partial^2 u}{\partial x^2} + \frac{\partial^2 u}{\partial y^2} + 2\mathrm{i}k\frac{\partial u}{\partial z} = 0. \tag{A2}$$

It is easy to verify that the solution of (A2) with the boundary conditions set on an inclined object is

$$u_1(x,y,z) = \exp\left[\mathrm{i}\alpha x + \mathrm{i}\beta y - \mathrm{i}\frac{\alpha^2+\beta^2}{2k}(z+a)\right], \tag{A3}$$

$$u(x = s\sin\theta, y, z = -a - s\cos\theta) = \exp(\mathrm{i}qs + \mathrm{i}py), \tag{A4}$$

where the quantities β and $\alpha = \alpha(q,p)$ are defined by the equations

$$\beta = p, \quad \alpha(q,p)\sin\theta + \frac{\alpha^2(q,p)+p^2}{2k}\cos\theta = q. \tag{A5}$$

The behaviour of an ideal lens in the three dimensional case can be described by a phase factor $T(x,y) = \exp[-\mathrm{i}k(x^2 + y^2)/(2f)]$, where f is the focal length, so that on the right side of the lens, the field has the form

$$u_2(x, y, z = 0) = u_1(x, y, z = 0)T(x, y). \tag{A6}$$

Within the framework of the paraxial approximation, the field on the right side of the lens can be found using the Fresnel integral:

$$u_2(x,y,z) = \frac{k}{2\pi \mathrm{i}z}\int_{-\infty}^{\infty}\int_{-\infty}^{\infty}\mathrm{d}x'\mathrm{d}y' u_2(x', y', z=0) \times \exp\left[\mathrm{i}k\frac{(x-x')^2+(y-y')^2}{2z}\right]. \tag{A7}$$

Substituting (A3) into (A6) and (A7), after performing the appropriate calculations and elementary transformations we obtain

$$u_2(x,y,z) = -\frac{1}{z/f-1}\exp\left[\mathrm{i}\frac{k(x^2+y^2)}{2f(z/f-1)}\right] \times \exp\left\{\frac{\mathrm{i}}{z/f-1}\left[-\alpha(q,p)x - py - \frac{\alpha^2(q,p)+p^2}{2k} \times a\left(\frac{1}{f}-\frac{1}{a}\right)\left(z - \frac{1}{1/f-1/a}\right)\right]\right\}. \tag{A8}$$

We rewrite (A5) in the form:

$$\alpha(q,p) = \frac{q}{\sin\theta} - \frac{\alpha^2(q,p)+p^2}{2k}\frac{1}{\tan\theta}. \tag{A9}$$

Substitute (A9) into (A8), we obtain

$$u_2(x,y,z) = -\frac{1}{z/f-1}\exp\left[\mathrm{i}\frac{k(x^2+y^2)}{2f(z/f-1)}\right] \times \exp\left\{\frac{\mathrm{i}}{z/f-1}\left\{-\frac{qx}{\sin\theta} - py + \frac{\alpha^2(q,p)+p^2}{2k\tan\theta} \times \left[-x - a\left(\frac{1}{f}-\frac{1}{a}\right)\left(z - \frac{1}{1/f-1/a}\right)\right]\right\}\right\}. \tag{A10}$$

Expression (A10) defines the field behind the lens in a form suitable for further consideration.

We now find the desired image, i.e. the field on a plane optically conjugated with the object plane. The equation of this plane is

$$x - (z - b)\tan\theta' = 0, \tag{A11}$$

where

$$\frac{1}{a} + \frac{1}{b} = \frac{1}{f}; \quad \tan\theta' = \frac{1}{M_0}\tan\theta; \quad M_0 = \frac{b}{a}. \tag{A12}$$

The equation for the plane (A11) can be written in the parametric form:

$$x(s') = -s'\sin\theta', \qquad y(y') = -y', \qquad z(s') = b - s'\cos\theta'. \tag{A13}$$

Let us substitute the parametric equation (A13) into (A10); in this case, the coefficient at $\alpha^2(q,p) + p^2$ in the exponent in (A10) will be, with allowance for (A12), equal to zero, and as a result we obtain

$$u(s',y') = u_2(x(s'), y(y'), z(s')) = \exp\left\{\mathrm{i}\frac{k[x^2(s')+y'^2]}{2f[z(s')/f-1]}\right\} \times [z(s')/f-1]^{-1}\exp\left\{\frac{\mathrm{i}qs'}{(\sin\theta/\sin\theta')[z(s')/f-1]} + \frac{\mathrm{i}py'}{z(s')/f-1}\right\}. \tag{A14}$$

Thus, the field of the object, specified as the product of the harmonics $\exp(\mathrm{i}qs + \mathrm{i}py)$, transforms into the field (A14). Consequently, the field of an arbitrary object

$$u_0(s,y) = \int_{-\infty}^{\infty}\int_{-\infty}^{\infty}\mathrm{d}q\mathrm{d}q U_0(q,p)\exp(\mathrm{i}qs + \mathrm{i}py) \tag{A15}$$

transforms in the image plane in the field having the form

$$u(s',y') = -\exp\left\{\mathrm{i}\frac{k[x^2(s')+y'^2]}{2f[z(s')/f-1]}\right\}[z(s')/f-1]^{-1} \times u_0\left(\frac{s'}{(\sin\theta/\sin\theta')[z(s')/f-1]}, \frac{y'}{z(s')/f-1}\right). \tag{A16}$$

This immediately implies relation (26) for the image field intensity $I(s', y') = |u(s', y')|^2$:

$$I(s', y') = \frac{1}{Q^2(s')} I_0\left(s^*(s'), \frac{y'}{Q(s')}\right).$$

References

1. Madou M. *Fundamentals of Microfabrication and Nanotechnology* (Boca Raton, FL: CRC Press, 2011) Vol. 2.
2. Pease R.F., Chou S.Y. *Proc. IEEE*, **96** (2), 248 (2008).
3. Wachulak P.W., Capeluto M.G., Marconi M.C., Menoni C.S., Rocca J.J. *Opt. Express*, **15** (6), 3465 (2007).
4. Li W., Marconi M.C. *Opt. Express*, **23** (20), 25532 (2015).
5. Pirati A., Smith D., Minnaert A., et al. *Proc. SPIE Int. Soc. Opt. Eng.*, **9422**, 94221P (2015).
6. Otsuka T., Li B., O'Gorman C., Cummins T., Kilbane D., Higashiguchi T., Yugami N., Jiang W., Endo A., Dunne P., O'Sullivan G. *Proc. SPIE Int. Soc. Opt. Eng.*, **8322**, 832214 (2012).
7. Hector S., Mangat P. *J. Vac. Sci. Technol., B*, **19** (6), 2612 (2001).
8. Andreev S.S., Bibishkin M.S., Chkhalo N.I., Kluenkov E.B., Prokhorov K.A., Salashchenko N.N., et al. *J. Synchrotron Radiat.*, **10** (5), 358 (2003).
9. Artyukov I.A., Mitrofanov A.N., Popov A.V., Vinogradov A.V. *Proc. of the 12th Int. Conf. on X-ray Lasers* (Berlin–Heidelberg: Springer-Verlag, 2010) pp 329–340.
10. Artyukov I.A., Busarov A.S., Popov N.L., Vinogradov A.V. *Proc. of the 13th Int. Conf. on X-Ray Lasers* (Paris, France: Springer Proceedings in Physics, 2014) Vol. 147, pp 19–27.
11. Papoulis A. *Systems and Transforms with Applications in Optics* (Malabar, FL: Krieger, 1981).
12. Rocca J. et al. *Phys. Rev. A*, **89**, 053820 (2014).
13. Hädrich S. et al. *Nat. Photonics*, **8**, 779 (2014).
14. Ribic P.R., Margaritondo G. *J. Phys. D: Appl. Phys.*, **45**, 213001 (2012).